JCI insight

Airway-resident memory CD4 T-cell activation accelerates antigen presentation and T-cell priming in draining lymph nodes

Caroline M. Finn, … , Tara M. Strutt, K. Kai McKinstry

JCI Insight. 2024. https://doi.org/10.1172/jci.insight.182615.

Research In-Press Preview **Immunology** **Inflammation**

Specialized memory CD4 T cells that reside long-term within tissues are critical components of immunity at portals of pathogen entry. In the lung, such tissue-resident memory (T_{RM}) cells are activated rapidly after infection and promote local inflammation to control pathogen levels before circulating T cells can respond. However, optimal clearance of Influenza A virus can require T_{RM} and responses by other virus-specific T cells that reach the lung only several days after their activation in secondary lymphoid organs. Whether local CD4 T_{RM} sentinel activity can impact the efficiency of T cell activation in secondary lymphoid organs is not clear. Here, we found that recognition of antigen by influenza -primed T_{RM} in the airways promotes more rapid migration of highly activated antigen-bearing dendritic cells to the draining lymph nodes. This in turn accelerated the priming of naive T cells recognizing the same antigen, resulting in newly activated effector T cells reaching the lungs earlier than in mice not harboring T_{RM}. Our findings thus reveal a circuit linking local and regional immunity whereby antigen recognition by T_{RM} improves effector T cell recruitment to the site of infection though enhancing the efficiency of antigen presentation in the draining lymph node.

Airway-resident memory CD4 T-cell activation accelerates antigen presentation and T-cell priming in draining lymph nodes

Caroline M. Finn[1], Kunal Dhume[1], Eugene Baffoe[1], Lauren A. Kimball[1], Tara M. Strutt[1], and K. Kai McKinstry[1,2]

[1] Burnett School of Biomedical Sciences, Division of Immunity and Pathogenesis
College of Medicine, University of Central Florida, Orlando, FL, USA

[2] Corresponding author:

K. Kai McKinstry, PhD
Email: kai.mckinstry@ucf.edu
Phone: 407-266-7137
Fax: 407-266-7002

Conflict of Interest Statement: The authors have declared that no conflicts of interest exist.

Abstract

Specialized memory CD4 T cells that reside long-term within tissues are critical components of immunity at portals of pathogen entry. In the lung, such tissue-resident memory (T_{RM}) cells are activated rapidly after infection and promote local inflammation to control pathogen levels before circulating T cells can respond. However, optimal clearance of Influenza A virus can require T_{RM} and responses by other virus-specific T cells that reach the lung only several days after their activation in secondary lymphoid organs. Whether local CD4 T_{RM} sentinel activity can impact the efficiency of T cell activation in secondary lymphoid organs is not clear. Here, we found that recognition of antigen by influenza -primed T_{RM} in the airways promotes more rapid migration of highly activated antigen-bearing dendritic cells to the draining lymph nodes. This in turn accelerated the priming of naive T cells recognizing the same antigen, resulting in newly activated effector T cells reaching the lungs earlier than in mice not harboring T_{RM}. Our findings thus reveal a circuit linking local and regional immunity whereby antigen recognition by T_{RM} improves effector T cell recruitment to the site of infection though enhancing the efficiency of antigen presentation in the draining lymph node.

Introduction

CD4 T cells can mediate strong protection against Influenza A virus (IAV through multiple mechanisms, even in the absence of preexisting neutralizing Ab (1-5). Furthermore, T cells can recognize proteins that are highly conserved across IAV strains, unlike key neutralizing Ab targets that rapidly mutate. There is thus enthusiasm for harnessing memory CD4 T cells as a component of improved IAV vaccine strategies able to provide 'universal' protection against diverse IAV strains (6-8). While some memory T cells circulate through the blood and lymphoid tissues, specialized tissue-resident memory T cells (T_{RM}) reside long-term at sites of previous infection and play key roles in immunosurveillance (9). Indeed, lung T_{RM} have been shown to contribute to optimal protection following challenges with diverse respiratory pathogens, including IAV (10-12). Virtually all studies centered on how T_{RM} impact outcomes focus on their ability to rapidly modulate the tissue environments in which they reside. During IAV infection, CD4 T_{RM} are activated by viral antigens within 40 h of viral exposure, which substantially precedes the activation of T cells recognizing IAV-derived peptides in secondary lymphoid organs (13, 14). This rapid T_{RM} response triggers a local inflammatory cascade that can control viral titers (13, 14) during what is otherwise the 'stealth phase' of IAV infection (15) which precedes the vigorous activation innate immune defenses.

While T_{RM} responses alone may be sufficient for T cell-mediated protection in some situations (16), IAV clearance has been shown in others to involve contributions from IAV-specific T_{RM} and from other IAV-specific T cells that reach the lung several days after infection (17-19). The efficient priming of new antiviral effector T cells recognizing the virus requires transport of IAV antigens by migratory dendritic cells (DC) from the lungs to the draining mediastinal lymph nodes (dLN) (20). It is unclear whether the activation of lung T_{RM} and of naive

T cells responding to IAV antigens in the dLN are independent processes, or if T_{RM} activation has impacts beyond those in the lung that impact the efficiency of T cell priming in secondary lymphoid organs. Understanding this relationship may lead to novel strategies for vaccines to better integrate local and regional T cell immunity against IAV and other respiratory pathogens.

Here, we investigated how recognition of antigen in the airways by IAV-primed lung CD4 T_{RM} regulates presentation of the antigen, and the activation of naive T cells recognizing the antigen, in secondary lymphoid organs. To do so, we gave cognate fluorescently-tagged protein, without additional adjuvant, intranasally (i.n.) to IAV-primed mice in order to recall a cohort of CD4 T_{RM} with known antigen-specificity. This approach allows for clear identification of the DC that take up the antigen in the lung (fluorescence$^+$ DC), as well for tracking antigen-bearing DC migration to secondary lymphoid organs (21). Importantly, this approach avoids triggering of pattern recognition receptors that are associated with infection that can independently promote DC activation (22) and pulmonary DC migration to secondary lymphoid organs (23). Furthermore, we analyzed impacts of lung CD4 T_{RM} activation on DC activation and migration in IAV-primed mice and in unprimed mice seeded with a physiological number of IAV-primed CD4 T_{RM} through i.n. transfer. Comparing outcomes in these two models allows for determination of how changes in the cellular landscape of the lung and dLN that are induced by IAV infection facilitate or constrain the impacts of CD4 T_{RM} recall on antigen presentation dynamics. These changes include epigenetic modifications in populations of innate immune cells in the lung, including antigen presenting cells like alveolar macrophages (24), the formation of inducible bronchus-associated lymphoid tissue, which may provide important niches for T_{RM} recall (25), and long-term changes in the cellularity of draining lymph nodes (dLN), which can impact T cell priming there (18, 26).

We show that antigen recognition by T_{RM} in IAV-primed mice and by T_{RM} in the airways of unprimed mice accelerates the activation and migration of antigen-bearing DC to the dLN. This improves the kinetics of priming of naive CD4 and CD8 T recognizing the i.n. administered antigen, which ultimately allows newly activated T effector cells to reach the lungs more quickly, an outcome that also requires CXCR3-dependent chemokine signals that are induced in the lung during T_{RM} activation. Furthermore, we show that these mechanisms can have an adjuvant-like impact in promoting new T cell responses in the lungs in response to levels of antigen that are too low to do so in mice not harboring T_{RM}. Finally, we show that airway CD4 T_{RM} activation likewise accelerates T cell priming and the recruitment of newly activated T cells to the lungs during virulent IAV infection. These findings indicate that CD4 T_{RM} activation has important consequences beyond the environment in which they respond that can dramatically improve T cell responses initiated in regional lymph nodes. Our results thus further underscore the benefits of targeting lung CD4 T_{RM} generation through vaccination to protect against respiratory viruses.

Results

Airway and interstitial lung T_{RM} are rapidly activated by airway antigen in IAV-primed mice

To investigate how antigen sensing by lung CD4 T_{RM} impacts antigen presentation in secondary lymphoid organs, we generated a T_{RM} cohort of known T cell receptor (TcR) specificity as in our previous studies addressing requirements for lung CD4 T_{RM} survival (27). We gave $1x10^6$ naive $CD90.1^+CD90.2^+$ OT-II TcR transgenic CD4 T cells intravenously (i.v.) to syngeneic $CD90.2^+$ B6 hosts and then primed the mice with a sublethal i.n. dose of the mouse-adapted IAV strain PR8-OVA_{II} that expresses a peptide of ovalbumin protein (OVA), which is recognized by the OT-II TcR (Figure 1A). The virus was delivered in a volume of 50uL, which preferentially targets infection to the lungs versus the upper airways (28). At 45 days post infection (dpi), most $CD90.1^+$ donor OT-II cells detected in the lung fit canonical CD4 T_{RM} criteria in that >90% were shielded from labeling by fluorescent anti-CD4 Ab given i.v. shortly before lung harvest, indicating their location in a niche that is inaccessible to the vasculature (29). Furthermore, the $i.v.^{shielded}$ population expressed higher levels of CD69, which is important for facilitating tissue retention by interfering with sphingosine-1-phospate dependent signaling that promotes tissue egress (30) (Figure 1B). The $CD69^{high}$ $i.v.^{shielded}$ phenotype is the most widely used discriminator of CD4 T_{RM} versus circulating ($CD69^{low}i.v.^{labeled}$) memory subsets across murine studies (31).

Lung T_{RM} can be divided based on location into those associated with the airways, that are recoverable by bronchoalveolar lavage (BAL), and interstitial T_{RM} that are not. About 25% of the $i.v.^{shieled}$ OT-II T_{RM} were recovered by BAL (Figure 1C). We performed phenotypic analysis to ask if the T_{RM} recovered by BAL represent a fraction of a relatively homogenous lung T_{RM} pool

versus a subset with distinct attributes from interstitial T_{RM}. Several markers that have been shown to discriminate T_{RM} from circulating memory cells were differentially expressed by interstitial and airway T_{RM} (Supplemental Fig 1). These included lower CD127 and higher CD49a expression by airway vs interstitial T_{RM}, both consistent with previous observations (32, 33). While interstitial T_{RM} expressed less Ly6C than circulating memory cells, consistent with recent observations (34), we found Ly6C to be even further reduced on airway T_{RM}. Levels of several adhesion molecules were also reduced on airway vs circulating T_{RM} including CD11a, CD49b, CD49d, which may be important in facilitating residency in this niche. Furthermore, airway T_{RM} expressed less CD5 than interstitial T_{RM}. CD5 expression by CD8 T cells may reflect sensitivity to IL-15 (35), suggesting that IL-15, which can sustain lung CD4 T_{RM} survival (27), may differentially impact T_{RM} in airway versus interstitial niches. Finally, while IFNγ production after restimulation of both T_{RM} subsets was similar, more interstitial T_{RM} produced IL-2, TNF, IL-17, and IL-10 (Supplemental Figure 1). These results indicate striking phenotypic and functional heterogeneity between IAV-primed airway and interstitial T_{RM}.

We next determined the kinetics of OT-II T_{RM} recall by cognate antigen introduced into the lower airways by giving 50 μg of OVA protein i.n. in 50uL of PBS. As controls, separate IAV-primed mice harboring T_{RM} received either 50 μg of BSA, which is not recognized by the OT-II TcR, or PBS alone. We assessed T_{RM} activation 6 h after OVA administration, a timepoint at which DC have been shown to efficiently present MHC-II-restricted peptides derived from protein antigens delivered by the s.c. route (36). Despite their higher constitutive expression of CD69 versus circulating OT-II memory cells, most T_{RM} further upregulated CD69, which is a commonly used early marker of T cell activation, and expressed higher levels of CD25, which is upregulated after CD69 following TcR triggering (Figure 1D). No signs of activation were

induced by i.n. instillation of BSA or PBS alone (Figure 1D). When analyzed separately, 70% of airway and 90% of interstitial T_{RM} upregulated CD69, with more interstitial than airway T_{RM} also upregulating CD25 **(**Figure 1E). These results demonstrate rapid recall of the majority of interstitial and airway T_{RM} in IAV-primed mice after cognate antigen delivery into the airways.

CD4 T_{RM} activation boosts numbers and activation of antigen-bearing DC in the dLN

To ask if antigen sensing by CD4 T_{RM} can regulate presentation of peptides derived from the antigen in secondary lymphoid organs, we gave 50 μg of OVA protein labeled with FITC (FITC-OVA) or FITC-BSA to IAV-primed mice harboring OT-II T_{RM} or to unprimed control mice. Monitoring the appearance of $FITC^+$ cells in secondary lymphoid organs after i.n. administration of FITC-tagged antigen is a well-established approach to identify migratory antigen presenting cells (21). While no $FITC^+$ cells were detected in the dLN 6 h post FITC-OVA administration (not shown), $FITC^+$ cells were detectable in the dLN by 20 h (Figure 2A). In contrast, no $FITC^+$ cells were detected at 20 h in the spleen or in the cervical lymph nodes, which drain the upper airways (37) (Figure 2A). The $FITC^+$ cells in the dLN at 20 h expressed a $CD45^+MHC\text{-}II^+CD11c^+B220^-SiglecF^-$ phenotype marking DCs (Supplemental Figure 2). Furthermore, the $FITC^+$ DC expressed higher levels of the chemokine receptor CCR7 than the $FITC^-$ DC present in the dLN (Figure 2B), consistent a migratory DC phenotype (38). About ~70% of the $FITC^+$ DC in the dLN were $CD11b^+CD103^-$ while the remainder were $CD11b^-CD103^+$ **(**Figure 2C**)**. These phenotypes fit criteria marking conventional DC2 and DC1 subsets, respectively (39), and are consistent the breakdown of $FITC^+$ migratory DC subsets seen in similar models (23, 40).

The frequency and number of FITC$^+$ DC detected in the dLNs of unprimed mice given FITC-OVA or FITC-BSA, and in IAV-primed mice given FITC-BSA, were all similar (Figure 2D). Strikingly, about 10-fold more FITC$^+$ DC were seen in IAV-primed mice given FITC-OVA (Figure 2D), but the proportion of FITC$^+$ DC1 vs DC2 was similar in primed vs unprimed mice receiving FITC-OVA (Figure 2E). To confirm that the increase in migratory DC in the dLN of primed mice receiving FITC-OVA was due to the presence of OVA-specific CD4 T_{RM}, we treated IAV-primed mice with CD4 depleting Ab prior to FITC-OVA administration to eliminate donor and any host OVA-specific memory CD4 cells generated by IAV priming. Thorough CD4 depletion in the lung via both intraperitoneal (i.p.) and i.n. Ab administration (Figure 2F, left) reduced FITC$^+$ DC detected in the dLN 20 h after FITC-OVA administration to numbers similar to those in unprimed mice (Figure 2F, right). To verify that FITC$^+$ cells were indeed presenting peptides derived from FITC-labeled antigen, we cultured naive OT-II cells in vitro with sort-purified FITC$^+$ or FITC$^-$ DCs from dLNs of mice given FITC-OVA. The OT-II cells were activated after 48 h, as evidenced by CD69 upregulation, when cultured with FITC$^+$ but not FITC$^-$ DCs, unless the FITC$^-$ DC were pulsed with OVA peptide prior to culture (Figure 2G).

We next asked if antigen recognition by T_{RM} impacts qualitative properties of the migratory DCs. Indeed, FITC$^+$ DC in IAV-primed mice given FITC-OVA vs FITC-BSA expressed higher levels of the costimulatory molecules CD40, CD80, and CD86 20 h after antigen administration (Figure 2H), reflecting an enhanced activation status. The two best characterized signals by which CD4 T cells impact APC activation are through CD40 ligand (CD40L) costimulation and IFNγ production (41, 42). However, Ab treatment to block CD40L prior to FITC-OVA administration did not impact the number of FITC$^+$ DCs in the dLN, while, unexpectedly, IFNγ-neutralizing Ab treatment increased FITC$^+$ DC numbers (Figure 2I). Type I IFN has also been implicated in

promoting DC activation (43, 44), but treatment with Ab to block the IFNα/β receptor (IFNAR-1) did not impact detection of $FITC^+$ DC in the dLN (Figure 2I). None of these treatments impacted CD40, CD80, or CD86 expression by $FITC^+$ DC, or the proportion of DC1 vs DC2 (data not shown). These findings indicate that lung CD4 T_{RM} activation accelerates antigen-bearing DC migration to the dLN, and boosts their activation status, independently of major pathways governing CD4 T cell-dependent APC regulation in other settings.

CD4 T_{RM} activation accelerates antigen-bearing DC activation in the lung

We next asked whether enhanced DC migration mediated by CD4 T_{RM} activation correlates with more rapid activation of antigen-bearing DC in the lung. We thus assessed $FITC^+$ DC in the lungs (see Supplemental Figure 2 for gating strategy) 6 h after FITC-OVA administration to unprimed mice, and in IAV-primed mice receiving FITC-OVA or FITC-BSA. This timepoint precedes $FITC^+$ DC migration to the dLN, but TcR-dependent T_{RM} activation is evident at 6 h (see Figure 1). While the proportion of DC1 vs DC2 within $FITC^+$ DC was similar in all groups (Figure 3A), more $FITC^+$ DC were detected in primed mice receiving FITC-OVA than in primed mice given FITC-BSA, and in unprimed mice given FITC-OVA (Figure 3B). Furthermore, the $FITC^+$ DC in lungs of primed mice receiving FITC-OVA expressed more CD40, CD80, and CD86 than in primed mice receiving FITC-BSA or in unprimed mice receiving FITC-OVA (Figure 3C). We also assessed $FITC^+$ DC in lungs of primed mice 6 h after receiving FITC-OVA that were depleted of $CD4^+$ cells as in Figure 2. Depletion decreased the number of $FITC^+$ DC (Figure 3D), and reduced their expression of CD40, CD80, and CD86 (Figure 3E). Antigen recognition by CD4 T_{RM} thus increases the number and activation status of antigen-bearing DC in the lung within 6 h of i.n. antigen exposure.

Airway CD4 T_{RM} activation in unprimed mice promotes enhanced antigen presentation in dLNs

IAV infection promotes structural changes and long-term alterations in the cellular landscapes of the lung (45-51) and dLN (18, 52). Aspects of these infection-driven changes could be required to facilitate T_{RM}-dependent impacts on antigen presentation in the dLN described above. We therefore asked the extent to which lung CD4 T_{RM} can regulate lung DC migration to the dLNs in unprimed mice. To do so, we isolated donor CD90.1$^+$ memory OT-II cells from the lungs of IAV-primed B6 mice at 21-28 dpi and transferred 1x10^6 i.n. to new unmanipulated CD90.2$^+$ B6 host mice in a 50 μL volume to target the lungs. To verify that this approach seeds a physiologically relevant number of T_{RM}, we compared the number of OT-II T_{RM} detected in the lungs of adoptive hosts 1 day after i.n. transfer **(**Figure 4A; open circle) to numbers of T_{RM} detected in the lungs of mice receiving naive OT-II cells prior to IAV priming as assessed from 14-60 dpi (Figure 4A, black circles). This analysis revealed a 'take' of i.n. transferred T_{RM} in unprimed host mice approximating the number of OT-II T_{RM} derived from naive donor cells in the lungs of IAV-primed mice at ~ 40 dpi.

We next compared the interstitial versus airway location of OT-II T_{RM} in IAV-primed mice at 45 dpi and of the OT-II T_{RM} in adoptive hosts one day after transfer using a FACS-based approach (4, 53). We gave one clone of anti-CD4 Ab i.v. and a non-competing anti-CD4 Ab clone with a different fluorescent tag i.n. shortly before lung harvest. This analysis identified that the majority of T_{RM} in IAV-primed mice were interstitial (i.n. Ab^{shieled}/i.v. Ab^{shielded}), with about 30% present in airway (i.n. Ab^{labeled}/i.v. Ab^{shielded}) niches **(**Figure 4B**)**, closely matching proportions based on BAL recovery shown in Figure 1. In contrast, virtually all i.n. transferred T_{RM} were associated with the airways (i.n. Ab^{labeled}/i.v. Ab^{shielded}) in adoptive hosts (Figure 4B). However,

only about two-thirds of the transferred T_{RM} could be recovered by BAL (Figure 4C), indicating that some T_{RM} rapidly seed an airway-associated niche after i.n. transfer (evidenced by i.n. Ab labeling) that is inaccessible to recovery by BAL.

To ask if the transferred T_{RM} remain localized to the lung, we first challenged mice receiving i.n. OT-II T_{RM} with a sublethal dose of PR8-OVA_{II} one day after cell transfer and enumerated donor cells present in the lung, dLN, and spleen at 7 dpi. Infection drove modest T_{RM} expansion in the lungs, but virtually no donor cells were detected in the dLN or spleen (Supplemental Fig 3), demonstrating locally restricted recall. We next assessed T_{RM} activation in adoptive hosts in response to i.n. delivery of 50 μg of FITC-OVA. The T_{RM} upregulated CD69 and CD25 within 6 h, with similar patterns seen for T_{RM} recovered by BAL or not (Figure 4D), matching the rapid kinetics of in situ OT-II T_{RM} recall shown in Figure 1.

CD4 T_{RM} activation in IAV-primed mice induces rapid induction of a broad array of innate inflammatory mediators in the lung (13, 14). To test if antigen sensing by the transferred T_{RM} could induce an inflammatory burst in unprimed mice, we assessed innate cytokines and chemokines in lung homogenates 20 h after i.n. FITC-OVA administration to B6 mice harboring OT-II T_{RM} or not. Levels of major inflammatory mediators including IFNγ, IL-6, CXCL9, CXCL10, CCL3, and CCL4, were at or near baseline in mice not harboring T_{RM}, but all were strikingly upregulated in T_{RM} recipients (Figure 4E). The inflammatory response in T_{RM} recipients correlated with higher numbers of several innate immune cell subsets in the lungs including neutrophils, NK cells, and γδT cells, that we previously showed to be activated by CD4 T_{RM} responses against IAV (13, 27), as well as NKT cells, while alveolar macrophages were unchanged (Figure 4F). Representative staining to identify these innate immune subsets is shown in Supplemental Figure 4. Recognition of protein antigen by IAV-primed CD4 T_{RM} in the airways

of unprimed mice thus recapitulates hallmarks of their protective in situ response during IAV infection.

We next asked if antigen sensing by airway CD4 T_{RM} in unprimed mice impacts DC migration to the dLN. About 2-fold more $FITC^+$ DC were detected in the lungs (Figure 4G) and about 5-fold more were detected in the dLN (Figure 4H) of T_{RM} recipients 20 h after FITC-OVA administration. Furthermore, the $FITC^+$ DCs in the dLNs of T_{RM} recipients expressed more CD40, CD80, and CD86 (Figure 4I). These results match the impacts of *in situ* T_{RM} recall in IAV-primed mice summarized earlier, and indicate that antigen sensing by airway CD4 T_{RM} can enhance regional antigen presentation in the absence of any longer-term infection-induced changes in the lung or dLN.

T_{RM}-enhanced antigen presentation improves T cell priming efficiency in the dLN

We next asked if the boosted efficiency of antigen presentation in the dLN mediated by CD4 T_{RM} activation can impact T cell priming. To do so, we transferred a cohort of naive CFSE-labeled $CD45.2^+CD90.2^+$ OT-II cells i.v. to $CD45.1^+$ B6 hosts with or without i.n. transfer of IAV-primed $CD90.1^+/CD90.2^+$ OT-II T_{RM}. This approach allows for differentiation of host ($CD45.1^+$), donor T_{RM} ($CD45.2^+CD90.2^+CD90.1^+$) and responders derived from naive donor cells ($CD45.2^+CD90.2^+CD90.1^-$). One day later, we gave 50 μg of FITC-OVA in 50 μL of PBS i.n. to both groups of mice and analyzed the cells derived from naive donor cells in the dLN after 3 days (Figure 5A). About 4-fold more naive responders were detected in T_{RM} recipients (Figure 5B). Furthermore, the cells derived from naive donors had divided more extensively based on loss of CFSE (Figure 5C), and expressed higher levels of the proliferation marker Ki67 (Figure 5D) than in mice not receiving T_{RM}.

To ask if airway CD4 T_{RM} activation can likewise enhance the kinetics of CD8 T cell priming, which requires cross-presentation in this model, we tracked responses of naïve $CD45.2^+CD90.2^+CD90.1^-$ donor OT-I TcR CD8 T cells in $CD45.1^+$ B6 mice receiving i.n. transfer of $CD45.2^+CD90.2^+CD90.1^+$ OT-II T_{RM} or not. The OT-I TcR recognizes a peptide of OVA restricted to $H\text{-}2K^b$ (54). More OT-I cells (Figure 5E) expressing higher levels of Ki67 (Figure 5F) were detected in mice harboring OT-II T_{RM}. Lung DCs can migrate from the dLN to the spleen after IAV infection to activate T cells there (55). However, while activated OT-I and OT-II cells were detected in the spleen, no differences in number were seen comparing mice harboring T_{RM} or not (Figure 5G). Enhanced presentation of airway antigens in the dLN mediated by CD4 T_{RM} activation thus promotes more rapid regional activation of naive CD4 and CD8 T cells.

Airway T_{RM} promote lung trafficking and enhanced functionality by newly activated T cells

We next asked if T_{RM}-dependent acceleration of naive T cell activation in the dLN impacts responses by newly primed T cells in the lungs using the same adoptive transfer approach to separate transferred naive and T_{RM} OT-II cells as described above (Figure 6A). While very few OT-II cells derived from naive donors were detected in the lungs 3 days after FITC-OVA administration in mice harboring T_{RM} or not, about 10-times more were present in T_{RM} recipients on day 4 **(**Figure 6B**)**. To ensure that i.n. OVA challenge generated functional effector cells, we assessed the cytokine production capacity of newly activated OT-II cells present in the lungs. Markedly more newly primed OT-II cells produced IFNγ in T_{RM} recipients, with higher frequencies of IFNγ/IL-2 double-positive cells, compared to newly primed cells in mice without T_{RM} (Figure 6C). CD4 T_{RM} recall also enhanced the number of OT-I effectors derived from naïve donors in the lungs after FITC-OVA challenge, though not as dramatically (Figure 6D). T_{RM} recall

did not significantly impact IFNγ production by OT-I effectors (Figure 6E), although a trend for more IFNγ$^+$ cells in mice harboring T_{RM} was seen across experiments.

We next titrated the amount of FITC-OVA given i.n. to ask if airway CD4 T_{RM} could promote new T cell responses in the lung against levels of antigen too low to stimulate lung infiltration otherwise. The T_{RM} were activated by a 100-fold lower dose of FITC-OVA (0.5 μg) than used in the experiments described above (0.5 μg) as assessed by upregulation of CD69 at 6 h, but not by 0.05 μg of FITC-OVA (Figure 6F). However, CD69 upregulation induced by 0.5 μg versus 50 μg of antigen was notably reduced. FITC$^+$ DC were not reliably detectable in the lung or dLN after 0.5 μg FITC-OVA administration, but about 4-fold more activated (CFSE^{low}Ki-67^{high}) cells derived from naive OT-II cells were seen in dLNs after 3 days in mice harboring T_{RM} (Figure 6G). Moreover, while effectors derived from naive OT-II donors were virtually absent from lungs of mice not receiving T_{RM}, they were readily detectable in T_{RM}-bearing mice after 4 days (Figure 6H).

We reasoned that CD4 T_{RM}-dependent chemokine signals may be required for the influx of new effectors into the lungs seen above. CXCR3-dependent chemokines promote T cell trafficking to the lung during IAV infection (56), and we detected rapid T_{RM}-dependent induction of CXCL9 and CXCL10 in the lungs of unprimed mice receiving FITC-OVA (see Figure 3). We therefore treated mice given T_{RM} and naive OT-II or OT-I cells with CXCR3-blocking or control Ab prior to i.n. administration of 0.5 μg of OVA and enumerated effectors derived from the naive donor cells in the lungs 4 days later. CXCR3 blockade reduced numbers of newly activated CD4 and CD8 T cells to the very low numbers seen in mice not receiving T_{RM} (Figure 6I**)**. These results establish a regional circuit, linked through the activation of airway CD4 $T_{RM,}$ that boosts the

efficiency by which T cells recognizing airway antigens are primed in the dLN and the chemokine-dependent recruitment of newly activated effector T cells to the lung.

Finally, we asked if we could see T_{RM}-dependent acceleration of naive T cell responses during IAV infection. To do so, we transferred naive CFSE-labeled CD90.2$^+$ OT-II cells i.v., with or without i.n. transfer of IAV-primed CD90.2$^+$CD90.1$^+$ OT-II T_{RM}, to unprimed CD45.1$^+$ mice as in the experiments above, then infected the mice with PR8-OVA_{II} (Figure 6J). We enumerated CFSE$^-$Ki67^{high} responders derived from the naive donor cells at 4 dpi (Figure 6K), a timepoint when antiviral CD4 T cell responses are not yet maximal in the dLN and when very few newly primed effector T cells are detected in the lungs during primary IAV infection. About 3-times more fully-divided Ki67^{high} effectors derived from naive donor cells were seen in the dLNs and in the lungs of mice harboring T_{RM}, but similar numbers were detected in the spleen (Figure 6L). These patterns match those seen assessing newly primed effector responses against FITC-OVA described above. Thus, even in the presence of infection-induced inflammation, airway CD4 T_{RM} activation can accelerate regional T cell priming and the appearance of newly activated effector T cells in the lungs.

Discussion

Virtually all investigation on how CD4 T_{RM} affect immune responses focuses on their local impacts in the tissues where they reside. For example, IAV-specific CD4 T_{RM} activation by viral antigen initiates a rapid inflammatory burst in the lungs resulting in the control of viral titers within 40 h of infection (13, 14). While this response may be sufficient to clear IAV in some settings (16), optimal T cell-dependent IAV clearance in other studies has been shown to require T_{RM} and virus-specific T cells that must be activated in secondary lymphoid organs before migrating to the lung (17, 18). We show here that, beyond coordinating local inflammatory environments, TcR-dependent CD4 T_{RM} activation can accelerate naive T cell priming by promoting faster migration of highly activated antigen-bearing DCs to the dLN, demonstrating another in way in which the adaptive immune system can regulate innate immunity (57). We suggest that aspects of control by CD4 T_{RM} on regional antigen presentation may be impactful and targetable in a wide array of settings beyond IAV infection. For example, protective synergies between CD4 T_{RM} and circulating T cells are described in mouse models using other pathogens including *Francisella tularensis* (58), *Chlamydia trachomatis* (59), and coronavirus (4). Linkages between tumor-resident and circulating T cells have also been described in models of cancer (60, 61). Negative impacts have also been reported for synergies between local and systemic T cells in contributing to disease in models of vitiligo (62) and house dust mite allergen-induced asthma (63). Investigation to determine the extent to which T_{RM}-mediated impacts on regional antigen presentation influence the activation and effector functions of circulating T cells in these varied situations may reveal novel approaches to improve outcomes.

We found similar enhancements in the number and activation status of antigen-bearing DCs in dLNs after delivery of cognate antigen to IAV-primed mice harboring OT-II T_{RM} and to

unprimed mice seeded with IAV-primed OT-II T_{RM}. While T_{RM} in IAV-primed mice could be divided into interstitial and airway compartments, all i.n. transferred T_{RM} were associated with the airways of their adoptive hosts. We thus conclude that airway-associated CD4 T_{RM} activation is sufficient to mediate the impacts on regional antigen presentation that we report, which is teleologically appealing as this location is on the frontline of antigen encounter. However, we further differentiated airway-associated T_{RM} in adoptive hosts into lavagable (labeled by i.v. administered Ab and recoverable by BAL) and non-lavagable (labeled by i.v. administered Ab but not recoverable by BAL) compartments. Diverse leukocytes have recently been identified in lavagable and non-lavagable airway niches in IAV-primed mice using a similar approach (64). Further studies are required to determine how the precise location of airway CD4 T_{RM} impacts their interaction with different subsets of cells to promote the outcomes we describe, as this could provide import insight for strategies aimed at targeting T_{RM} persistence in specific lung microenvironments to maximize their impacts. Most of the cytokines and chemokines that we found upregulated in lung homogenates of T_{RM}-bearing mice after i.n. FITC-OVA administration were also detected previously in supernatants of cultured lung CD4 T_{RM} and cognate peptide-bearing DC (27). This supports the hypothesis that initial T_{RM}-DC interactions serve as a 'spark' to promote a broader lung inflammatory cascade (65). Here, we show that these same interactions also have consequences outside of the lung through promoting enhanced presentation of airway antigens in the dLN.

We found both CD4 and CD8 T cell priming in the dLN to be accelerated after T_{RM} recognition of airway antigens. This correlated with improved migration of antigen-bearing DC2 and DC1 from the lung to the dLN. These DC subsets are associated with preferential activation of $CD4^+$ and $CD8^+$ T cells, respectively (66). Unexpectedly, blockade of IFNγ increased the

number of migratory DC detected in the dLN of mice harboring OT-II T_{RM}. Negative regulation of DC migration by IFNγ has been seen in other settings, correlating with enhanced CCR5-dependent chemotaxis by the DCs (67). Given that T_{RM} activation boosted levels of IFNγ and of CCR5 ligands (CCL3 and CCL4) in the lungs, we speculate that these signals may act to limit DC egress. Such regulation may be important to facilitate robust cognate interactions between antigen-bearing DC and effector T cells arriving in the lung during infection. Indeed, interactions with DC have been shown to be important for effector T cells in the lung to mediate antiviral activity (68), and can promote cytotoxic CD4 T cell differentiation during IAV infection (69). Notably, we found the number of $FITC^+$ DC detected in the lung 6 h after i.n. FITC-OVA administration was reduced following depletion of OT-II CD4 T cells. While it is possible that this outcome may in part be due to depletion of $CD4^+$ DC (70), that more $FITC^+$ DC were also seen in in the lungs mice harboring OT-II T_{RM} following i.n. delivery of FITC-OVA versus FITC-BSA suggests that cognate interactions with T_{RM} may provide important survival signals to antigen-bearing DC. Indeed, MHC-II expression by DC has been found to support the survival of peptide-pulsed DC in vivo in other settings (71).

We found CD4 T_{RM} activation to boost costimulatory molecule expression by antigen-bearing DCs independently of IFNγ and CD40L signals using Ab treatments based on previous experiments of ours in which these Ab clones were found to impact outcomes of IAV infection (72). Nevertheless, a limitation of the work presented here is that we cannot rule out the possibility that the Ab-mediated neutralization of these signals was incomplete. However, we previously showed that CD4 T_{RM}-mediated control of IAV titers is independent of IFNγ, CD40, and type I IFN signaling using mice knockout mouse models (13), which supports the findings in this report that T_{RM}-mediated control of DC migration is likewise independent of these signals. CD40L-

independent DC activation by T cells has been reported by others (73), and may require strong TcR-mediated interactions (74). In contrast to our findings, IFNγ was found to be critical for CD4 T_{RM}-dependent protection, and optimal DC migration from infected lungs to dLNs in a mouse model of coronavirus infection (4). These discrepancies indicate that key functional requirements may differ during CD4 T_{RM} responses against different respiratory viruses. However, shared programming across infections may underlie the establishment and survival of lung CD4 T_{RM} in airway and interstitial niches. This is supported by our findings that phenotypic markers distinguishing airway and interstitial T_{RM} in IAV-primed mice, including CD11a, CD27, CD49d, CD127, and Ly6C, were also found to differentiate corona virus-specific CD4 T_{RM} in these niches (4). Most T_{RM} primed by viral infection fit Th1 criteria, but protective Th17-polarized IAV-specific T_{RM} have been described (75), and dominant Th2 (76, 77) and Th17 (78, 79) lung T_{RM} are seen in other settings. Whether such T_{RM} can also accelerate regional antigen presentation, and if so, whether conserved or unique signals are involved across Th-polarization states, are important questions for future study.

We found that the number of IAV-primed lung CD4 T_{RM} drop about 50-fold from 21 to 60 dpi, and similar rates of decline have been reported for IAV-primed CD8 T_{RM} (80). Thus, even with optimal T_{RM} priming through vaccination or infection, the timeframe during which enough lung T_{RM} are present to successfully combat a given dose of IAV without contributions from circulating T cells may be of limited duration. Indeed, we previously showed that a relatively high number, $3x10^6$, of i.n. transferred IAV-primed OT-II T_{RM} could protect unprimed hosts against a lethal dose of PR8-OVA_{II} while $1x10^6$ T_{RM} could not (27). Here, we show that i.n. transfer of $1x10^6$ IAV-primed OT-II T_{RM} is, however, sufficient to accelerate regional antigen presentation and to establish chemokine gradients needed to recruit newly activated T cells to the lung. That a

number of T_{RM} beneath the threshold required to promote protection is nevertheless able to accelerate regional T cell responses is consistent with the concept that the mechanisms described likely grow in importance in situations where T_{RM} recall must be augmented with antiviral T cells from systemic reservoirs. Indeed, newly primed antiviral T cells can be key contributors to IAV clearance even when high numbers of memory cells are responding as evidenced by experiments in which transferred IAV-specific memory CD4 T cells were shown to protect WT but not T cell-deficient hosts against the same IAV challenge dose (72).

Masopust and colleagues have shown that chemokine induction following CD8 T_{RM} activation can recruit unstimulated memory T cells to sites of infection where they can be activated locally (81). Our finding demonstrating that CD4 T_{RM} activation improves the kinetics of antigen delivery to the dLN, leading to faster T cell priming and the earlier appearance of new effector T cells in the lungs reveal a separate way in which T_{RM} can promote influx of protective T cells into tissues. Our preliminary studies also indicate that circulating memory T cell activation kinetics are similarly enhanced in the dLN following T_{RM} activation in this model (Finn and McKinstry, unpublished). Thus, incorporating CD4 T_{RM} into IAV vaccine strategies may help to accelerate both primary T cell responses against newly encountered viral antigens while also promoting faster recall of circulating memory T cells in the dLN that target conserved viral epitopes. In this regard, investigating whether CD4 T_{RM} in upper airways, another clinically relevant niche (82), can similarly impact regional T cell responses is important.

Finally, while our results show that antigen recognition by CD4 T_{RM} can improve regional T cell priming during virulent IAV infection, we speculate that the CD4 T_{RM}-dependent impacts we describe may be especially impactful in situations where APC activation is not triggered robustly though pattern recognition receptors, or when levels of antigen and inflammation are very

low. Indeed, that CD4 T_{RM} can promote lung responses by naive T cells against levels of antigen in the airways too low to do so otherwise indicates that CD4 T_{RM} act as extremely sensitive amplifiers of low-end antigenic stimuli. This adjuvant-like impact of CD4 T_{RM} may be highly beneficial in non-infectious settings, for example in adoptive immunotherapy against cancers. Further study to test this possibility and to define the full scope of outcomes impacted by this mode of regulation may lead to new ways that CD4 T_{RM} can be harnessed to prevent or manage disease in the respiratory tract and other tissue sites.

Methods

Sex as a biological variable

Our study examined male and female animals, and similar findings are reported for both sexes.

Mice

Wildtype C57BL/6J (B6) mice or CD45.1$^+$ B6 mice (JaxBoy) were used as hosts in all experiments at 8-12 weeks of age. For adoptive transfer experiments, CD45.2$^+$CD90$^+$ OT-II mice, CD45.2$^+$CD90.1$^+$CD90.2$^+$ OT-II mice, or CD45.2$^+$CD90.2$^+$ OT-I mice, all on a B6 background, were used at 4–8-weeks of age as a source of donor CD4 or CD8 T cells, respectively. The OT-II TcR recognizes aa 323-339 of OVA in the context of I-A^b (83), while the OT-I TcR recognizes aa 257-264 of OVA in the context of H-2K^b (54). All mice were originally obtained from Jackson Laboratories, and all strains other than the OT-I mice were bred at the Lake Nona Vivarium at the University of Central Florida.

Naive T cell isolation, adoptive transfers, and IAV infection

Naive CD8$^+$ or CD4$^+$ cells from unmanipulated OT-I or OT-II mice, respectively, were obtained from pooled spleen and peripheral lymph nodes that were gently pressed through a nylon membrane to make a single-cell suspension. Single-cell suspensions were incubated on nylon wool (Polysciences) for 1 h at 37 °C to enrich for T cells followed by Percoll (MilliporeSigma) gradient separation to isolate small resting lymphocytes. Positive MACS selection using CD8 or CD4 microbeads (Miltenyi Biotec) was then performed to isolate OT-I or OT-II cells, respectively.

The resulting cells were routinely >95% $CD8^+$ or $CD4^+$ and expressed a naive phenotype ($CD62L^{high}$, $CD44^{low}$). In some experiments, donor cells were labeled with CFSE (ThermoFisher) prior to injection into host mice in order to track cell division (84).

To generate OT-II T_{RM}, $CD90.2^+$ B6 mice received $1x10^6$ naive $CD90.1^+CD90.2^+$ OT-II cells in 200 μL of PBS by i.v. or retro-orbital (r.o.) injection. The mice were infected on the same day with an i.n. installation of a sublethal (0.2 LD_{50}) dose of the mouse-adapted IAV strain PR8-OVA_{II} in 50 μL of PBS under isoflurane anesthesia. The same dose of PR8-OVA_{II} was used for experiments tracking responses OT-II cell responses against IAV. The viral stock was originally characterized at the Trudeau Institute (Saranac Lake, NY) and expresses the epitope of OVA recognized by the OT-II TcR in the hemagglutinin protein (85). All infected mice were monitored daily for infection-induced morbidity, including weight loss, hunched posture, ruffled fur, and reduced movement; mice were euthanized if humane endpoints were reached.

Donor $CD90.1^+CD90.2^+$ OT-II cells were re-isolated from the lungs of PR8-OVA_{II}-primed $CD90.2^+$ B6 mice between 21 and 28 dpi as follows. Lung lobes were rinsed in PBS and then minced with a sterile razor blade and placed into C-tubes (Miltenyi) followed by digestion and homogenization using the mouse lung disassociation kit and a GentleMACS tissue dissociator with heaters (Miltenyi) as per the manufacter's instructions. This was followed by isolation of live lymphocytes by Lympholyte gradient separation (Cedarlane). The cells were filtered extensively followed by positive selection of the donor cells using CD90.1 MACS beads. The number of donor cells was determined by flow cytometry, with purity generally >85%, with < 3% contaminating $CD90.1^-CD90.2^+$ cells. The OT-II T_{RM} were transferred to new host mice under isoflurane anesthesia by i.n. instillation in 50 μL of PBS.

To track T cell responses against OVA, $5x10^5$ naive $CD90.2^+$ CD4 or CD8 T cells obtained from OT-II or OT-I TcR transgenic mice, respectively, were transferred via r.o. injection to $CD45.1^+$ B6 mice that also received T_{RM} or not through i.n. transfer one day prior to OVA challenge.

OVA administration, and in vivo Ab treatment

OVA, BSA, FITC-OVA, or FITC-BSA protein (ThermoFisher) was administered to mice by i.n. instillation in 50 μL of PBS under isoflurane anesthesia. All antigen stocks contained < 0.03 endotoxin units/mL as determined by Pierce gel clot endotoxin assay (ThermoFisher). In some experiments, mice were treated with anti-CD40L (clone MR-1; Bioxcell), anti-IFNγ (XMG1.2; Bioxcell), anti-type I IFN receptor (MAR1-583; Bioxcell) or isotype control Ab via i.p. injection of 250 μg in 200 μL of PBS one day prior to OVA administration, and 100 μg of Ab i.n. together with OVA administration. In other experiments, mice were treated with 250 μg of anti-CD4 Ab (GK1.5; Bioxcell) i.p. one day prior to OVA administration and 100 μg delivered i.n. together with OVA administration.

In some experiments, anesthetized IAV-primed mice were injected i.v. with 3μg of APC-labeled anti-CD4 Ab (GK1.5, Biolegend) in 100 μl of PBS with or without 1.5 μg of PE-labeled anti-CD4 (RM4.4, Biolegend) i.n. in 50 μL of PBS prior to euthanasia and organ harvest. GK1.5 and RM4.4 are non-competing clones in terms of binding CD4.

Tissue collection

All experimental mice were euthanized by cervical dislocation. For assessment of responses to airway antigens, exsanguination was performed by perforation of the abdominal aorta and lung perfusion by injection of PBS through the right ventricle of the heart. Lungs, spleen, and lymph nodes were harvested into RMPI 1640 media (Gibco) supplemented with 7.5% fetal bovine serum (Hyclone), 2mM L-glutamine (Gibco), 100 IU penicillin and 100 μg/mL streptomycin (Gibco), 10 mM HEPES (Gibco), 50 μM 2-mercaptoethanol (MilliporeSigma). Lymph nodes were prepared into single cell suspensions using an optimized mechanical disruption protocol by gentle and thorough pressing through a taut stainless-steel mesh (80 uM) using a sterile rubber plunger from a 5mL syringe. The mesh and plunger were then rinsed with 3 mL of media. This procedure was repeated 3 times. Spleen and Lung were processed by enzymatic digestion using a gentleMACS dissociator and enzyme kits specific for the lung or for spleen (Miltenyi) to generate single cell suspensions. All single cell suspensions were filtered through a 70 μM nylon cell strainer (Fisher) prior to further analysis.

In some experiments bronchoalveolar lavage (BAL) was collected by administering 1 ml of sterile PBS into the lungs via the exposed trachea and then gently retracting the fluid. This process was repeated 3 times per mouse, pooling the volume.

In some experiments $CD45^{+}MHC\text{-}II^{+}B220\text{-}CD11c^{+}$ cells were sort purified from the dLNs of mice one day after i.n. FITC-OVA administration using a CytoFlex SRT sorter (Beckman Coulter) into $FITC^{+}$ and $FITC^{-}$ populations. Some $FITC^{-}$ cells were pulsed with 10 μg/mL of OT-II peptide directly after sorting. All sorted APC populations were cocultured 1:1 with naive OT-II cells for 48 h prior to analysis of OT-II cells for CD69 expression by flow cytometry.

Flow cytometry

Single-cell suspensions were washed, resuspended in FACS buffer (PBS plus 0.5% BSA and 0.02% sodium azide), and incubated on ice with 1 μg of CD16/CD32 blocking Ab (2.4G2; Bioxcell) and optimized concentrations of the following fluorochrome-labeled Abs for surface staining. From Biolegend, anti-CD45.2 (104, PE-Cy7), anti-CD49a (HMα1, APC), anti-Ly-6C (HK1.4, FITC), anti-CD25 (PC61, PE), anti-MHC II (M5/114.15.2, PerCP), anti-CD11c (N418, efluor-450), anti-siglecF (E50-2440, APC-Cy7), anti-CD64 (S18017D, APC), anti-CD40 (3/23, APC), anti-CD80 (16-10A, PE), anti-CD86 (GL-, PE), anti-NK1.1 (PK136). From BD Biosciences, anti-CD11a (2D7, FITC), anti-CD49d (9C10, PE), anti-CD44 (IM7, PE), anti-B220 (RA3-6B2, BrilliantViolet-450), and from R&D anti-CXCR6 (221002, PE), anti-siglecF (E50-2440). From Thermo Fisher Scientific, anti-CD90.1 (HIS51, PerCP),anti-CD90.2 (53-2.1, efluor-450), anti-CD4 (RM4.5, PE), anti-CD8 (53-6.7, PE), anti-CD127 (sb/199), anti-CD27 (A7R34, APC), anti-CXCR3 (CXCR3-173, FITC, anti-CD69 (H1.2F3, PE), anti-CD62L (MEL-14, APC), anti-CCR7 (4B12, PE), anti-CD103 (2E7, PE), anti-GR-1 (RB6-8C5), anti-γδTCR (eBioGL3), anti-CD3 (17A2) and anti-CD11b (M1/70, APC). For intracellular cytokine staining, cells were stimulated for 4h with 10ng/ml PMA (MilliporeSigma) and 50ng/ml ionomycin (MilliporeSigma), and 10mg/ml brefeldin A (MilliporeSigma) added after 2 h. Cells were then surface stained and fixed for 20 min in 4% paraformaldehyde followed by permeabilization for 10 minutes in 0.1% saponin buffer (PBS plus 1% FBS, 0.1% NaN3, and 0.1% saponin). The cells were then stained for cytokine by the addition of fluorescently labeled anti-IFN-g (XMG1.2; ThermoFisher) and anti-IL-2 (JES6- 5H4; ThermoFisher) Abs for 20 min. Detection of Ki67 (SolA15, ThermoFisher) was conducted using the Foxp3 staining buffer set (ThermoFisher). Zombie NIR Fixable Viability kit (Biolegend) was used to discriminate live from dead cells.

All FACS analysis was performed using BD FACSCanto II (BD Biosciences) or Cytoflex (Beckman Coulter) flow cytometers and FlowJo (BD Biosciences) analysis software.

Detection of pulmonary cytokines and chemokines

Levels of cytokines and chemokines in lung homogenates collected as described previously (13) were determined using mouse multiplex kits (MilliporeSigma) read on a Bio-Plex Multiplex 200 Luminex reader (Bio-Rad).

Statistical analysis

Unpaired, two-tailed Student t tests were used to assess whether the means of two normally distributed groups differed significantly. The Welch correction was applied when variances were found to differ. One-way ANOVA analysis with appropriate multiple comparison posttest was used to compare multiple means. Significance is indicated as *$p<0.05$, **$p < 0.005$, ***$p < 0.001$, and ****$p < 0.0001$. All error bars represent SD. Statistical analysis was performed using GraphPad Prism software (GraphPad Software).

Study approval

All experimental animal procedures were approved by and conducted in accordance with the University of Central Florida's Animal Care and Use Committee's guidelines under protocol number 202300114.

Data availability

Values for all data points in graphs are reported in the Supporting Data Values file.

Author Contributions

C.M.F. and K.K.M contributed to conception, experimental design, and analysis, interpretation of data, and prepared the manuscript. C.M.F., E.B., L.A.K., and K.D. contributed to data acquisition. T.M.S. contributed to data acquisition, interpretation of data, and manuscript preparation.

Acknowledgements

We thank the University of Central Florida Lake Nona Vivarium staff for excellent care of the mice and the UCF flow cytometry core facility. This work was supported by NIH grants R21AI148882 and R01AI167994 (to KKM), NIH grant R01AI165406 (to T.M.S.), by a University of Central Florida Doctoral Support Award (to C.M.F.), and by a Solomon Klotz Excellence in Immunology and Allergy Award (to C.M.F.).

Competing Interests

The authors declare no competing interests.

References

1. Wilkinson TM, Li CK, Chui CS, Huang AK, Perkins M, Liebner JC, et al. Preexisting influenza-specific CD4+ T cells correlate with disease protection against influenza challenge in humans. *Nat Med.* 2012;18(2):274-80.
2. McIlwain DR, Chen H, Rahil Z, Bidoki NH, Jiang S, Bjornson Z, et al. Human influenza virus challenge identifies cellular correlates of protection for oral vaccination. *Cell Host Microbe.* 2021;29(12):1828-37 e5.
3. Valkenburg SA, Li OTW, Li A, Bull M, Waldmann TA, Perera LP, et al. Protection by universal influenza vaccine is mediated by memory CD4 T cells. *Vaccine.* 2018;36(29):4198-206.
4. Zhao J, Zhao J, Mangalam AK, Channappanavar R, Fett C, Meyerholz DK, et al. Airway Memory CD4(+) T Cells Mediate Protective Immunity against Emerging Respiratory Coronaviruses. *Immunity.* 2016;44(6):1379-91.
5. Finn CM, and McKinstry KK. Ex Pluribus Unum: The CD4 T Cell Response against Influenza A Virus. *Cells.* 2024;13(7).
6. Koutsakos M, Illing PT, Nguyen THO, Mifsud NA, Crawford JC, Rizzetto S, et al. Human CD8(+) T cell cross-reactivity across influenza A, B and C viruses. *Nat Immunol.* 2019;20(5):613-25.
7. Fox A, Quinn KM, and Subbarao K. Extending the Breadth of Influenza Vaccines: Status and Prospects for a Universal Vaccine. *Drugs.* 2018;78(13):1297-308.

8. Sant AJ. The Way Forward: Potentiating Protective Immunity to Novel and Pandemic Influenza Through Engagement of Memory CD4 T Cells. *J Infect Dis.* 2019;219(Suppl_1):S30-S7.

9. Christo SN, Park SL, Mueller SN, and Mackay LK. The Multifaceted Role of Tissue-Resident Memory T Cells. *Annu Rev Immunol.* 2024;42(1):317-45.

10. Zheng MZM, and Wakim LM. Tissue resident memory T cells in the respiratory tract. *Mucosal Immunol.* 2022;15(3):379-88.

11. Zhang M, Li N, He Y, Shi T, and Jie Z. Pulmonary resident memory T cells in respiratory virus infection and their inspiration on therapeutic strategies. *Front Immunol.* 2022;13:943331.

12. Cheon IS, Son YM, and Sun J. Tissue-resident memory T cells and lung immunopathology. *Immunol Rev.* 2023;316(1):63-83.

13. Strutt TM, McKinstry KK, Dibble JP, Winchell C, Kuang Y, Curtis JD, et al. Memory CD4+ T cells induce innate responses independently of pathogen. *Nat Med.* 2010;16(5):558-64, 1p following 64.

14. Chapman TJ, Lambert K, and Topham DJ. Rapid reactivation of extralymphoid CD4 T cells during secondary infection. *PLoS ONE.* 2011;6(5):e20493.

15. Moltedo B, Lopez CB, Pazos M, Becker MI, Hermesh T, and Moran TM. Cutting edge: stealth influenza virus replication precedes the initiation of adaptive immunity. *J Immunol.* 2009;183(6):3569-73.

16. Zens KD, Chen JK, and Farber DL. Vaccine-generated lung tissue-resident memory T cells provide heterosubtypic protection to influenza infection. *JCI Insight.* 2016;1(10).

17. Strutt TM, McKinstry KK, Kuang Y, Bradley LM, and Swain SL. Memory CD4+ T-cell-mediated protection depends on secondary effectors that are distinct from and superior to primary effectors. *Proc Natl Acad Sci U S A.* 2012;109(38):E2551-60.

18. Paik DH, and Farber DL. Influenza infection fortifies local lymph nodes to promote lung-resident heterosubtypic immunity. *J Exp Med.* 2021;218(1).

19. Suarez-Ramirez JE, Chandiran K, Brocke S, and Cauley LS. Immunity to Respiratory Infection Is Reinforced Through Early Proliferation of Lymphoid T(RM) Cells and Prompt Arrival of Effector CD8 T Cells in the Lungs. *Front Immunol.* 2019;10:1370.

20. GeurtsvanKessel CH, Willart MA, van Rijt LS, Muskens F, Kool M, Baas C, et al. Clearance of influenza virus from the lung depends on migratory langerin+CD11b- but not plasmacytoid dendritic cells. *J Exp Med.* 2008;205(7):1621-34.

21. Vermaelen KY, Carro-Muino I, Lambrecht BN, and Pauwels RA. Specific migratory dendritic cells rapidly transport antigen from the airways to the thoracic lymph nodes. *J Exp Med.* 2001;193(1):51-60.

22. Iwasaki A, and Pillai PS. Innate immunity to influenza virus infection. *Nat Rev Immunol.* 2014;14(5):315-28.

23. Jakubzick C, Helft J, Kaplan TJ, and Randolph GJ. Optimization of methods to study pulmonary dendritic cell migration reveals distinct capacities of DC subsets to acquire soluble versus particulate antigen. *J Immunol Methods.* 2008;337(2):121-31.

24. Xing Z, Afkhami S, Bavananthasivam J, Fritz DK, D'Agostino MR, Vaseghi-Shanjani M, et al. Innate immune memory of tissue-resident macrophages and trained innate immunity: Re-vamping vaccine concept and strategies. *J Leukoc Biol.* 2020;108(3):825-34.

25. Schreiner D, and King CG. CD4+ Memory T Cells at Home in the Tissue: Mechanisms for Health and Disease. *Front Immunol.* 2018;9:2394.

26. Stolley JM, Scott MC, O'Flanagan SD, Kunzli M, Matson CA, Weyu E, et al. Cutting Edge: First Lung Infection Permanently Enlarges Lymph Nodes and Enhances New T Cell Responses. *J Immunol.* 2024;212(11):1621-5.

27. Strutt TM, Dhume K, Finn CM, Hwang JH, Castonguay C, Swain SL, et al. IL-15 supports the generation of protective lung-resident memory CD4 T cells. *Mucosal Immunol.* 2018;11(3):668-80.

28. Flano E, Jewell NA, Durbin RK, and Durbin JE. Methods used to study respiratory virus infection. *Curr Protoc Cell Biol.* 2009;Chapter 26:Unit 26 3.

29. Anderson KG, Mayer-Barber K, Sung H, Beura L, James BR, Taylor JJ, et al. Intravascular staining for discrimination of vascular and tissue leukocytes. *Nat Protoc.* 2014;9(1):209-22.

30. Szabo PA, Miron M, and Farber DL. Location, location, location: Tissue resident memory T cells in mice and humans. *Sci Immunol.* 2019;4(34).

31. Kunzli M, and Masopust D. CD4(+) T cell memory. *Nat Immunol.* 2023;24(6):903-14.

32. Shen CH, Ge Q, Talay O, Eisen HN, Garcia-Sastre A, and Chen J. Loss of IL-7R and IL-15R expression is associated with disappearance of memory T cells in respiratory tract following influenza infection. *J Immunol.* 2008;180(1):171-8.

33. Chapman TJ, and Topham DJ. Identification of a unique population of tissue-memory CD4+ T cells in the airways after influenza infection that is dependent on the integrin VLA-1. *J Immunol.* 2010;184(7):3841-9.

34. Stolley JM, Johnston TS, Soerens AG, Beura LK, Rosato PC, Joag V, et al. Retrograde migration supplies resident memory T cells to lung-draining LN after influenza infection. *J Exp Med.* 2020;217(8).

35. Choi YJ, Lee H, Kim JH, Kim SY, Koh JY, Sa M, et al. CD5 Suppresses IL-15-Induced Proliferation of Human Memory CD8(+) T Cells by Inhibiting mTOR Pathways. *J Immunol.* 2022;209(6):1108-17.

36. Itano AA, McSorley SJ, Reinhardt RL, Ehst BD, Ingulli E, Rudensky AY, et al. Distinct dendritic cell populations sequentially present antigen to CD4 T cells and stimulate different aspects of cell-mediated immunity. *Immunity.* 2003;19(1):47-57.

37. Randall TD, and Mebius RE. The development and function of mucosal lymphoid tissues: a balancing act with micro-organisms. *Mucosal Immunol.* 2014;7(3):455-66.

38. Marsland BJ, Battig P, Bauer M, Ruedl C, Lassing U, Beerli RR, et al. CCL19 and CCL21 induce a potent proinflammatory differentiation program in licensed dendritic cells. *Immunity.* 2005;22(4):493-505.

39. Cabeza-Cabrerizo M, Cardoso A, Minutti CM, Pereira da Costa M, and Reis e Sousa C. Dendritic Cells Revisited. *Annu Rev Immunol.* 2021;39:131-66.

40. Matthews KE, Karabeg A, Roberts JM, Saeland S, Dekan G, Epstein MM, et al. Long-term deposition of inhaled antigen in lung resident CD11b-CD11c+ cells. *Am J Respir Cell Mol Biol.* 2007;36(4):435-41.

41. Elgueta R, Benson MJ, de Vries VC, Wasiuk A, Guo Y, and Noelle RJ. Molecular mechanism and function of CD40/CD40L engagement in the immune system. *Immunol Rev.* 2009;229(1):152-72.

42. Hivroz C, Chemin K, Tourret M, and Bohineust A. Crosstalk between T lymphocytes and dendritic cells. *Crit Rev Immunol.* 2012;32(2):139-55.

43. Montoya M, Schiavoni G, Mattei F, Gresser I, Belardelli F, Borrow P, et al. Type I interferons produced by dendritic cells promote their phenotypic and functional activation. *Blood.* 2002;99(9):3263-71.

44. Gressier E, Schulte-Schrepping J, Petrov L, Brumhard S, Stubbemann P, Hiller A, et al. CD4(+) T cell calibration of antigen-presenting cells optimizes antiviral CD8(+) T cell immunity. *Nat Immunol.* 2023;24(6):979-90.

45. Kaur M, Bell T, Salek-Ardakani S, and Hussell T. Macrophage adaptation in airway inflammatory resolution. *Eur Respir Rev.* 2015;24(137):510-5.

46. Wu Q, Jorde I, Kershaw O, Jeron A, Bruder D, Schreiber J, et al. Resolved Influenza A Virus Infection Has Extended Effects on Lung Homeostasis and Attenuates Allergic Airway Inflammation in a Mouse Model. *Microorganisms.* 2020;8(12).

47. Wimmers F, Donato M, Kuo A, Ashuach T, Gupta S, Li C, et al. The single-cell epigenomic and transcriptional landscape of immunity to influenza vaccination. *Cell.* 2021;184(15):3915-35 e21.

48. Debisarun PA, Gossling KL, Bulut O, Kilic G, Zoodsma M, Liu Z, et al. Induction of trained immunity by influenza vaccination - impact on COVID-19. *PLoS Pathog.* 2021;17(10):e1009928.

49. Seo SU, and Seong BL. Prospects on Repurposing a Live Attenuated Vaccine for the Control of Unrelated Infections. *Front Immunol.* 2022;13:877845.

50. Hwang JY, Randall TD, and Silva-Sanchez A. Inducible Bronchus-Associated Lymphoid Tissue: Taming Inflammation in the Lung. *Front Immunol.* 2016;7:258.

51. Marin ND, Dunlap MD, Kaushal D, and Khader SA. Friend or Foe: The Protective and Pathological Roles of Inducible Bronchus-Associated Lymphoid Tissue in Pulmonary Diseases. *J Immunol.* 2019;202(9):2519-26.

52. Anthony SM, Van Braeckel-Budimir N, Moioffer SJ, van de Wall S, Shan Q, Vijay R, et al. Protective function and durability of mouse lymph node-resident memory CD8(+) T cells. *Elife.* 2021;10.

53. van de Wall S, Crooks S, Varga SM, Badovinac VP, and Harty JT. Cutting Edge: Influenza-Induced CD11alo Airway CD103+ Tissue Resident Memory T Cells Exhibit Compromised IFN-gamma Production after In Vivo TCR Stimulation. *J Immunol.* 2023;210(8):1025-30.

54. Hogquist KA, Jameson SC, Heath WR, Howard JL, Bevan MJ, and Carbone FR. T cell receptor antagonist peptides induce positive selection. *Cell.* 1994;76(1):17-27.

55. Jenkins MM, Bachus H, Botta D, Schultz MD, Rosenberg AF, Leon B, et al. Lung dendritic cells migrate to the spleen to prime long-lived TCF1(hi) memory CD8(+) T cell precursors after influenza infection. *Sci Immunol.* 2021;6(63):eabg6895.

56. Dhume K, Finn CM, Strutt TM, Sell S, and McKinstry KK. T-bet optimizes CD4 T-cell responses against influenza through CXCR3-dependent lung trafficking but not functional programming. *Mucosal Immunol.* 2019;12(5):1220-30.

57. Cronkite DA, and Strutt TM. The Regulation of Inflammation by Innate and Adaptive Lymphocytes. *J Immunol Res.* 2018;2018:1467538.

58. Roberts LM, Wehrly TD, Ireland RM, Crane DD, Scott DP, and Bosio CM. Temporal Requirement for Pulmonary Resident and Circulating T Cells during Virulent Francisella tularensis Infection. *J Immunol.* 2018;201(4):1186-93.

59. Nguyen N, Guleed S, Olsen AW, Follmann F, Christensen JP, and Dietrich J. Th1/Th17 T cell Tissue-Resident Immunity Increases Protection, But Is Not Required in a Vaccine Strategy Against Genital Infection With Chlamydia trachomatis. *Front Immunol.* 2021;12:790463.

60. Enamorado M, Iborra S, Priego E, Cueto FJ, Quintana JA, Martinez-Cano S, et al. Enhanced anti-tumour immunity requires the interplay between resident and circulating memory CD8(+) T cells. *Nat Commun.* 2017;8:16073.

61. Gitto S, Natalini A, Antonangeli F, and Di Rosa F. The Emerging Interplay Between Recirculating and Tissue-Resident Memory T Cells in Cancer Immunity: Lessons Learned From PD-1/PD-L1 Blockade Therapy and Remaining Gaps. *Front Immunol.* 2021;12:755304.

62. Richmond JM, Strassner JP, Rashighi M, Agarwal P, Garg M, Essien KI, et al. Resident Memory and Recirculating Memory T Cells Cooperate to Maintain Disease in a Mouse Model of Vitiligo. *J Invest Dermatol.* 2019;139(4):769-78.

63. Sethi GS, Gracias D, and Croft M. Contribution of circulatory cells to asthma exacerbations and lung tissue-resident CD4 T cell memory. *Front Immunol.* 2022;13:951361.

64. Chang MY, Brune JE, Black M, Altemeier WA, and Frevert CW. Multicompartmental analysis of the murine pulmonary immune response by spectral flow cytometry. *Am J Physiol Lung Cell Mol Physiol.* 2023;325(4):L518-L35.

65. Strutt TM, McKinstry KK, and Swain SL. Control of innate immunity by memory CD4 T cells. *Adv Exp Med Biol.* 2011;780:57-68.

66. Chudnovskiy A, Pasqual G, and Victora GD. Studying interactions between dendritic cells and T cells in vivo. *Curr Opin Immunol.* 2019;58:24-30.

67. Wu X, Hou W, Sun S, Bi E, Wang Y, Shi M, et al. Novel function of IFN-gamma: negative regulation of dendritic cell migration and T cell priming. *J Immunol.* 2006;177(2):934-43.

68. Cabeza-Cabrerizo M, Minutti CM, da Costa MP, Cardoso A, Jenkins RP, Kulikauskaite J, et al. Recruitment of dendritic cell progenitors to foci of influenza A virus infection sustains immunity. *Sci Immunol.* 2021;6(65):eabi9331.

69. Devarajan P, Vong AM, Castonguay CH, Silverstein NJ, Kugler-Umana O, Bautista BL, et al. Cytotoxic CD4 development requires CD4 effectors to concurrently recognize local antigen and encounter type I IFN-induced IL-15. *Cell Rep.* 2023;42(10):113182.

70. Vremec D, Pooley J, Hochrein H, Wu L, and Shortman K. CD4 and CD8 expression by dendritic cell subtypes in mouse thymus and spleen. *J Immunol.* 2000;164(6):2978-86.

71. Matthews KE, Qin JS, Yang J, Hermans IF, Palmowski MJ, Cerundolo V, et al. Increasing the survival of dendritic cells in vivo does not replace the requirement for CD4+ T cell help during primary CD8+ T cell responses. *J Immunol.* 2007;179(9):5738-47.

72. McKinstry KK, Strutt TM, Kuang Y, Brown DM, Sell S, Dutton RW, et al. Memory CD4+ T cells protect against influenza through multiple synergizing mechanisms. *J Clin Invest.* 2012;122(8):2847-56.

73. Ferrer IR, Liu D, Pinelli DF, Koehn BH, Stempora LL, and Ford ML. CD40/CD154 blockade inhibits dendritic cell expression of inflammatory cytokines but not costimulatory molecules. *J Immunol.* 2012;189(9):4387-95.

74. Ruedl C, Kopf M, and Bachmann MF. CD8(+) T cells mediate CD40-independent maturation of dendritic cells in vivo. *J Exp Med.* 1999;189(12):1875-84.

75. Omokanye A, Ong LC, Lebrero-Fernandez C, Bernasconi V, Schon K, Stromberg A, et al. Clonotypic analysis of protective influenza M2e-specific lung resident Th17 memory cells reveals extensive functional diversity. *Mucosal Immunol.* 2022.

76. Rahimi RA, Nepal K, Cetinbas M, Sadreyev RI, and Luster AD. Distinct functions of tissue-resident and circulating memory Th2 cells in allergic airway disease. *J Exp Med.* 2020;217(9).

77. Bosnjak B, Kazemi S, Altenburger LM, Mokrovic G, and Epstein MM. Th2-T(RMs) Maintain Life-Long Allergic Memory in Experimental Asthma in Mice. *Front Immunol.* 2019;10:840.

78. Shenoy AT, Wasserman GA, Arafa EI, Wooten AK, Smith NMS, Martin IMC, et al. Lung CD4(+) resident memory T cells remodel epithelial responses to accelerate neutrophil recruitment during pneumonia. *Mucosal Immunol.* 2020;13(2):334-43.

79. Amezcua Vesely MC, Pallis P, Bielecki P, Low JS, Zhao J, Harman CCD, et al. Effector T(H)17 Cells Give Rise to Long-Lived T(RM) Cells that Are Essential for an Immediate Response against Bacterial Infection. *Cell.* 2019;178(5):1176-88 e15.

80. Slutter B, Van Braeckel-Budimir N, Abboud G, Varga SM, Salek-Ardakani S, and Harty JT. Dynamics of influenza-induced lung-resident memory T cells underlie waning heterosubtypic immunity. *Sci Immunol.* 2017;2(7).

81. Schenkel JM, Fraser KA, Vezys V, and Masopust D. Sensing and alarm function of resident memory CD8(+) T cells. *Nat Immunol.* 2013;14(5):509-13.

82. Ramirez SI, Faraji F, Hills LB, Lopez PG, Goodwin B, Stacey HD, et al. Immunological memory diversity in the human upper airway. *Nature.* 2024;632(8025):630-6.

83. Barnden MJ, Allison J, Heath WR, and Carbone FR. Defective TCR expression in transgenic mice constructed using cDNA-based alpha- and beta-chain genes under the control of heterologous regulatory elements. *Immunol Cell Biol.* 1998;76(1):34-40.

84. Lyons AB, and Parish CR. Determination of lymphocyte division by flow cytometry. *J Immunol Methods.* 1994;171(1):131-7.

85. Thomas PG, Brown SA, Yue W, So J, Webby RJ, and Doherty PC. An unexpected antibody response to an engineered influenza virus modifies CD8+ T cell responses. *Proc Natl Acad Sci U S A.* 2006;103(8):2764-9.

Figures and Legends:

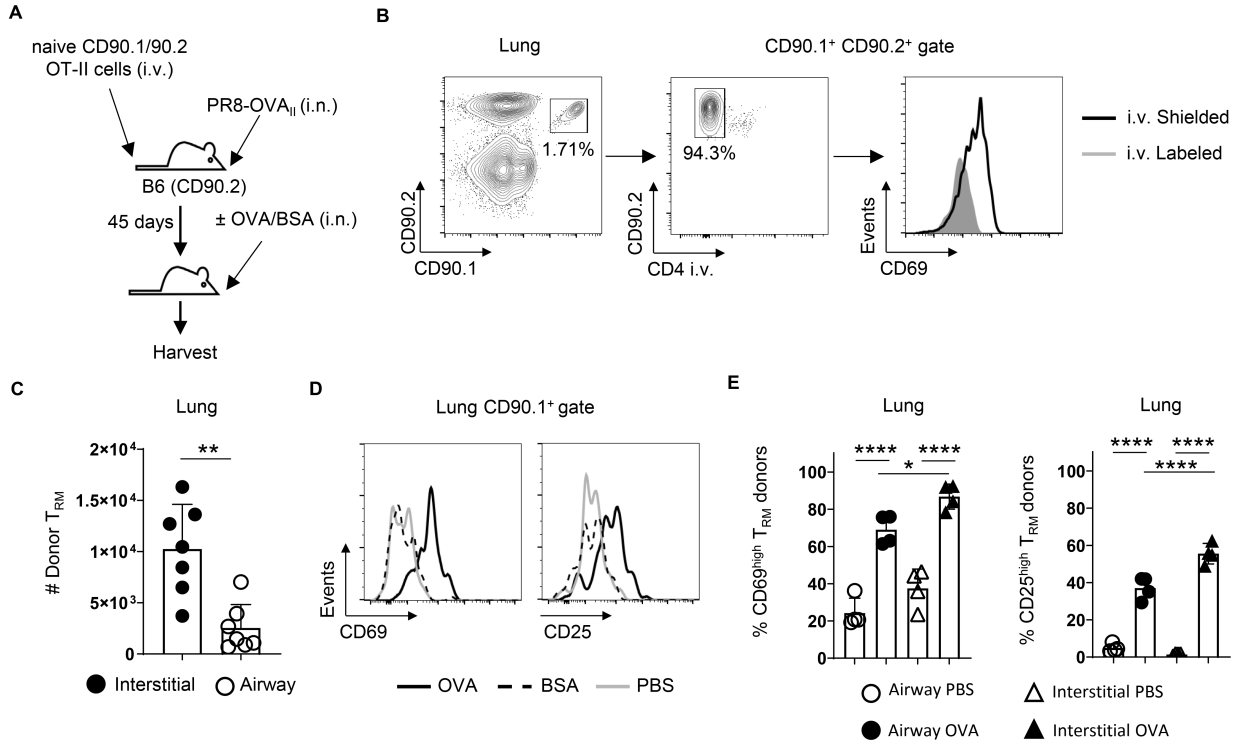

Figure 1: *IAV-primed lung CD4 T_{RM} respond rapidly to i.n. administered antigen.* **(A)** B6 mice received 1x10^6 naive CD90.1/CD90.2 OT-II cells i.v. followed by priming with PR8-OVA$_{II}$. After 45 days, the primed mice were challenged with i.n. administered antigen to recall OT-II T_{RM} in the lung. **(B)** Primed mice were treated at 45 dpi with fluorescent anti-CD4 Ab i.v. prior to lung harvest, with representative staining shown to identify donor OT-II cells (left), donor T_{RM} shielding from labeling by i.v. administered CD4 Ab (center), and expression of CD69 by the i.v.^{shielded} vs i.v.^{labeled} OT-II cells (right). **(C)** Number of donor T_{RM} (i.v.^{shielded}) cells in interstitial and airway niches based on BAL harvest; n = 7/group; pooled from 2 experiments. **(D)** IAV-primed mice were given 50 μg of OVA or BSA, or PBS alone via i.n. administration.

Representative CD69 (left) and CD25 (right) staining of total lung OT-II T_{RM} 6 h later. **(E)** The percentage of $CD69^{high}$ (left) and $CD25^{high}$ (right) donor T_{RM} in airway (circles) and interstitial (triangle) niches from separate mice given OVA or PBS: n=4-5 per group; results from 1 of 3 experiments. Students t-test used for pairwise comparison for (C) and one-way ANOVA with Tukey's multiple comparison was used in (E).

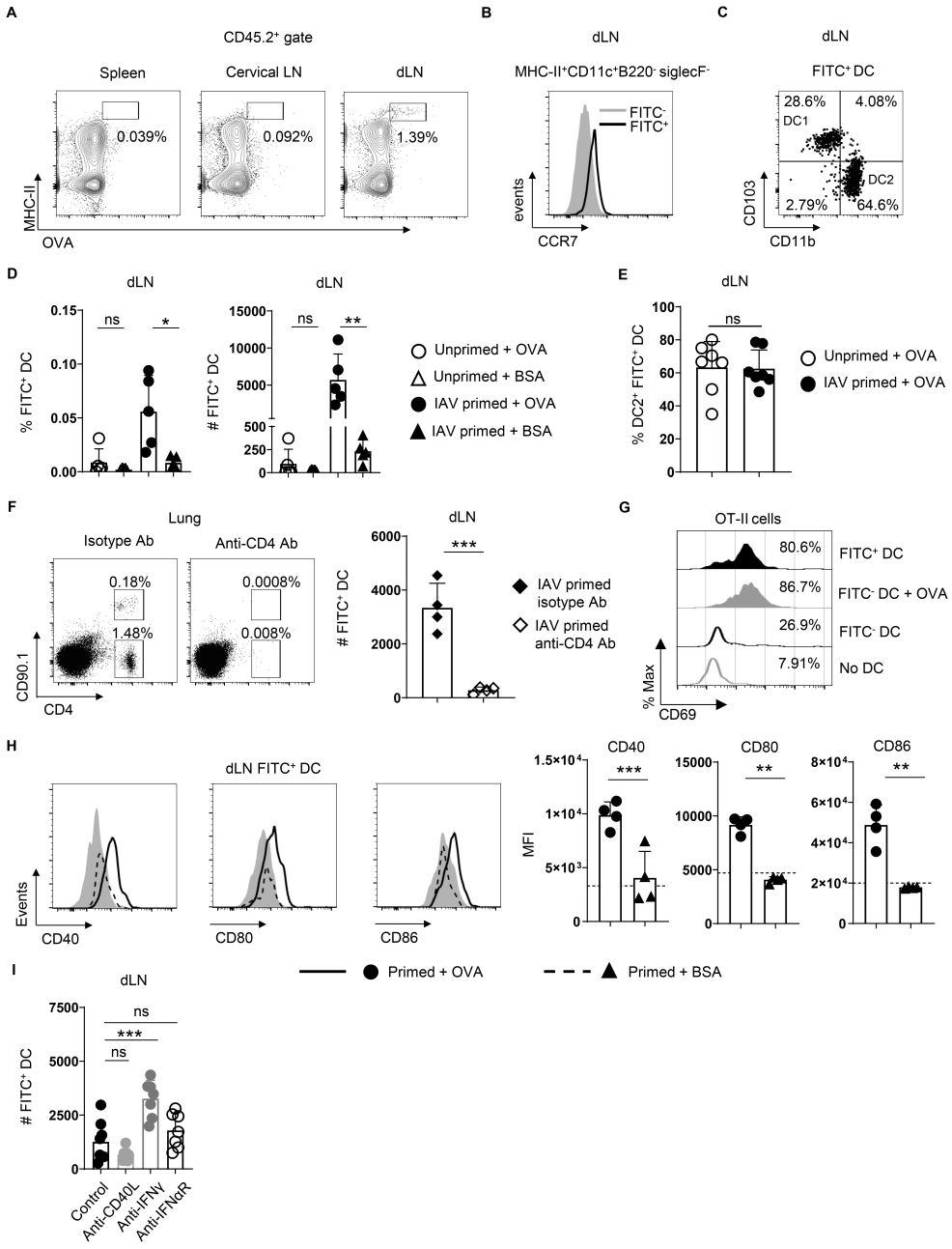

Figure 2: *Lung CD4 T_{RM} activation enhances the number and activation status of antigen-bearing DC in the dLN.* **(A)** Representative staining of FITC$^+$MHC-II$^+$ cells in stated organs 20 h after FITC-OVA administration to IAV-primed mice harboring OT-II T_{RM}. **(B)** Representative CCR7 expression by FITC$^+$ and FITC$^-$ DC and **(C)** CD11b and CD103 expression by FITC$^+$ DC to define

DC1 and DC2 subsets. **(D)** frequency (left) and number (right) of $FITC^+$ DC from stated mice 20 h after antigen administration; n=5/group; 1 of 2 experiments. **(E)** Frequency of DC2 within $FITC^+$ DC of primed and unprimed mice receiving FITC-OVA; n = 7; results pooled from 2 experiments. **(F)** Representative staining of donor and host CD4 T cells in lungs of primed mice receiving FITC-OVA and isotype or CD4-depleting Ab treatment (left) and the number of $FITC^+$ DC in the dLNs (right); n=4/group; 1 of 2 experiments. **(G)** CD69 expression by naive OT-II cells 48 h after culture with stated subsets of sort-purified DC from IAV-primed mice 20 h after FITC-OVA administration, with the percentage of $CD69^+$ cells averaged from triplicate wells; 1 of 3 experiments. **(H)** Representative staining and MFI of CD40, CD80, and CD86 expression by $FITC^+$ DC in dLNs of primed mice after FITC-OVA or FITC-BSA administration, with shaded histograms and dotted lines in graphs for expression in mice receiving PBS; n = 4 per group; results from 1 of 3 experiments. **(I)** Numbers of $FITC^+$ DC in dLNs 20 h after FITC-OVA administration to IAV-primed mice treated with stated Abs; n=7/group; pooled results from 2 of 3 experiments. Students t-test was used for pairwise comparison for all panels except (I) where one-way ANOVA with Dunnet's multiple comparison test was used.

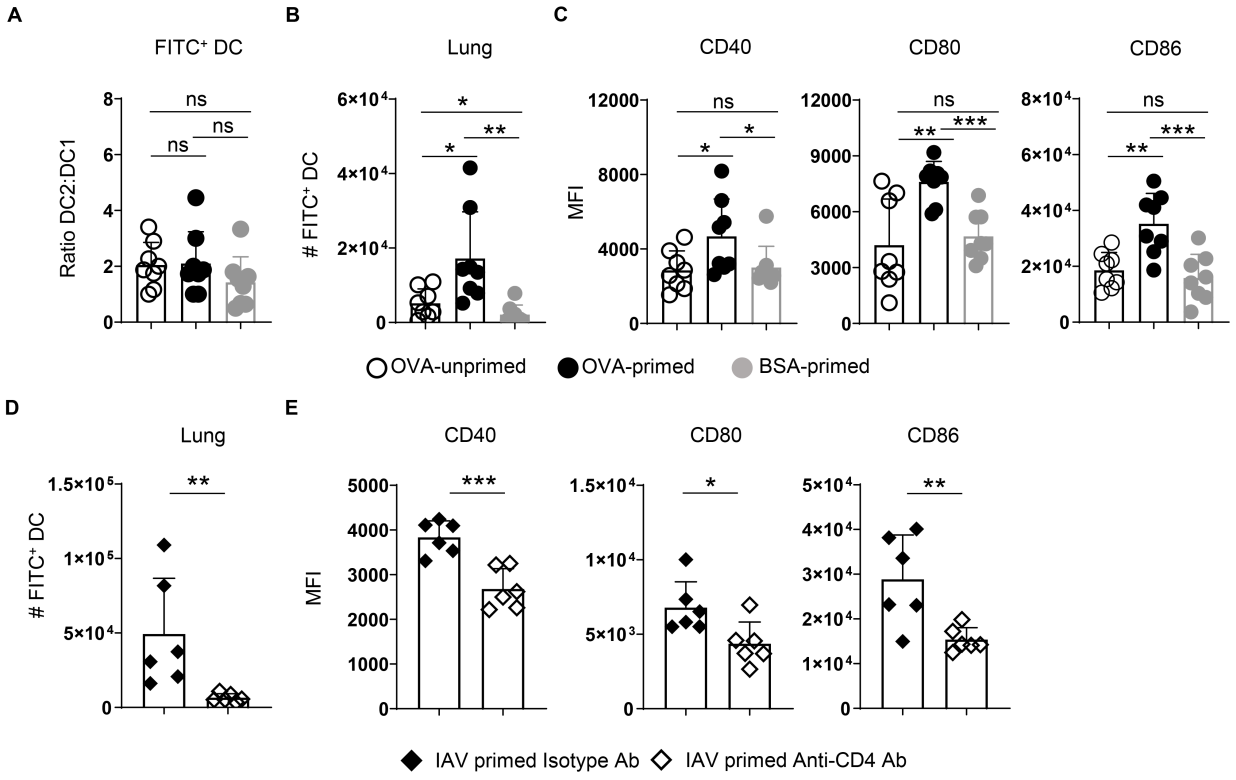

Figure 3: *Rapid activation of lung DC presenting cognate antigen by CD4 T_{RM}.* IAV-primed mice harboring OT-II T_{RM} or unprimed control mice were given 50 µg of FITC-OVA or FITC-BSA i.n. at 45 dpi. **(A)** The ratio of DC2 to DC1 within $FITC^+$ APC, **(B)** the number of total $FITC^+$ DC in the lungs of stated mice 6 h after antigen administration; and **(C)** MFI analysis of CD40, CD80 and CD86 expression by $FITC^+$ lung DC in stated groups; n =8/group; pooled from 2 experiments. **(D)** The number of $FITC^+$ lung DC and **(E)** their expression of CD40, CD80 and CD86 6 h after FITC-OVA administration to IAV-primed mice treated with isotype or CD4-depleting Ab; n = 6/group; results pooled from 2 experiments. One-way ANOVA with Tukey's multiple comparison was used in (E) in panels A-C; Students t-test was used for pairwise comparison in panels D and E.

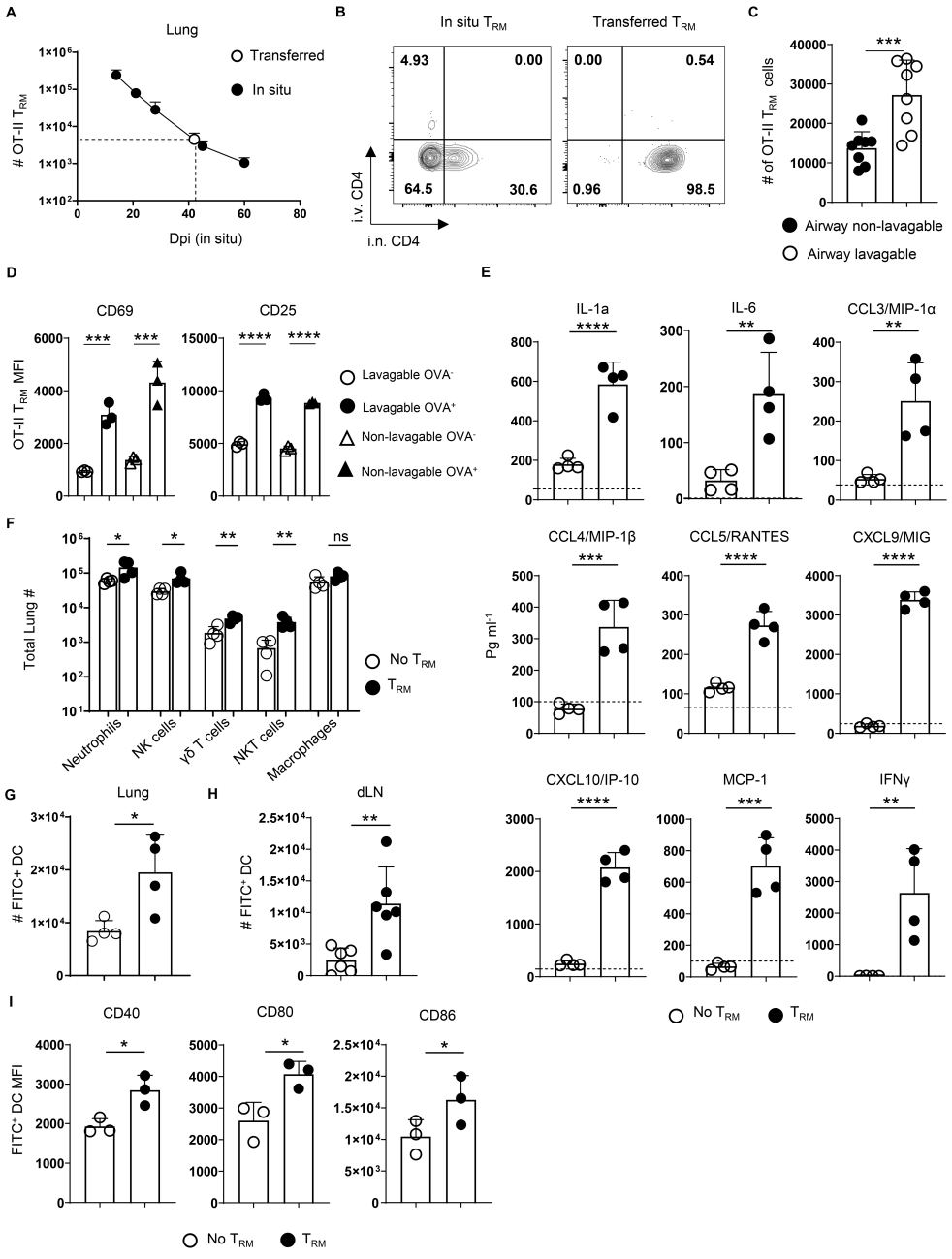

Figure 4: *IAV-primed CD4 T_{RM} rapidly respond to antigen in adoptive host mice after i.n. transfer*. **(A)** The number of OT-II T_{RM} in mice receiving naïve OT-II cells i.v. on stated days post-IAV priming (black) and the number of OT-II T_{RM} in unprimed host mice one day after i.n. transfer of OT-II memory cells isolated from lungs of IAV-primed mice (open); n=3 mice/group/timepoint.

(B) Representative labeling of lung OT-II memory cells in primed mice at 45 dpi (left) and donor OT-II T_{RM} in host mice 1 d after transfer (right) by non-competing anti-CD4 Ab clones given i.n. and i.v. before lung harvest and **(C)** number of non-lavagable and lavagable donor T_{RM} from unprimed host mice 1 day after transfer; n=8/group; pooled from 2 experiments. **(D)** CD69 (left) and CD25 (right) expression by donor T_{RM} subsets 6 h after i.n. administration of FITC-OVA or PBS alone; n=3-4/group; 1 of 3 experiments. **(E)** Levels of stated analytes in lung homogenates from mice receiving T_{RM} or not 20 h after FITC-OVA administration; dotted lines are average levels from mice receiving PBS alone; n = 4/group; 1 of 3 experiments. **(F)** Numbers of stated cell types in lungs of mice harboring T_{RM} or not 20 h after FITC-OVA administration; n=4/group; 1 of 2 experiments. Numbers of $FITC^+$ DC in **(G)** lungs (n =4/group; 1 of 2 experiments) and **(H)** dLN (n =6/group; pooled from 2 experiments) 20 h after FITC-OVA administration to unprimed mice harboring OT-II T_{RM} or not. **(I)** CD40, CD80, and CD86 expression by $FITC^+$ DC in the dLN; n=3/group; 1 of 3 experiments. Students t-test was used for pairwise comparison in all panel except (D) where one-way ANOVA with Tukey's multiple comparison was used.

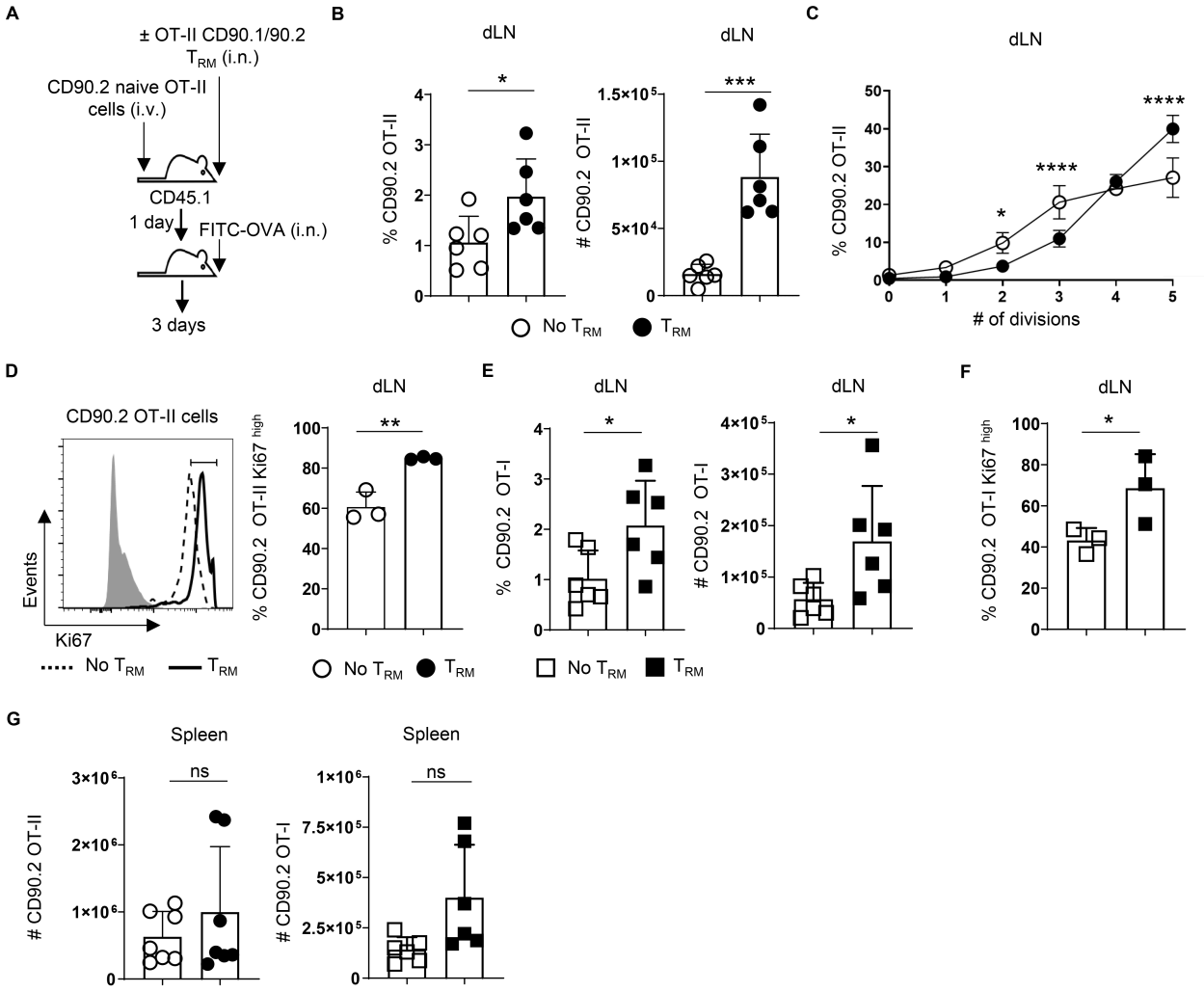

Figure 5: *Airway T_{RM} activation improves priming of naive T cells in dLNs.* **(A)** CD45.1$^+$ B6 mice received 1x10^6 naive CFSE-labeled CD90.2$^+$ OT-II cells i.v. with or without i.n. transfer of 1x10^6 CD90.1$^+$CD90.2$^+$ OT-II T_{RM}. All mice were then challenged i.n. with 50 μg of FITC-OVA. **(B)** Frequency (left) and number (right) of cells derived from naive CD90.2$^+$ OT-II donors in dLNs after 3 days; n=7; pooled from 2 experiments, with **(C)** analysis of CFSE dilution (n=4/group; 1 of 3 experiments) and **(D)** representative Ki-67 staining from naive OT-II responders, with bulk host T cells as shaded histogram (left), and the frequency of Ki-67^{high} responders (right) from individual mice (n=3/group; 1 of 3 experiments). **(E)** Frequency (left) and number (right) of

responding cells derived from naïve OT-I cells donor cells in the dLN of mice harboring OT-II T_{RM} or not 3 d after FITC-OVA administration; n=6/group; pooled from 2 experiments. **(F)** Frequency of $Ki67^{high}$ OT-I cells in dLNs of mice harboring T_{RM} or not; n=3; 1 of 2 experiments. **(G)** Number of cells derived from naïve OT-II (left) and OT-I (right) cells in the spleens of mice harboring T_{RM} or not 3 days after i.n. FITC-OVA administration; n =7/group for OT-II and 6/group for OT-I; results pooled from 2 experiments each with OT-II and OT-I cells. Students t-test was used for pairwise comparison in all panels.

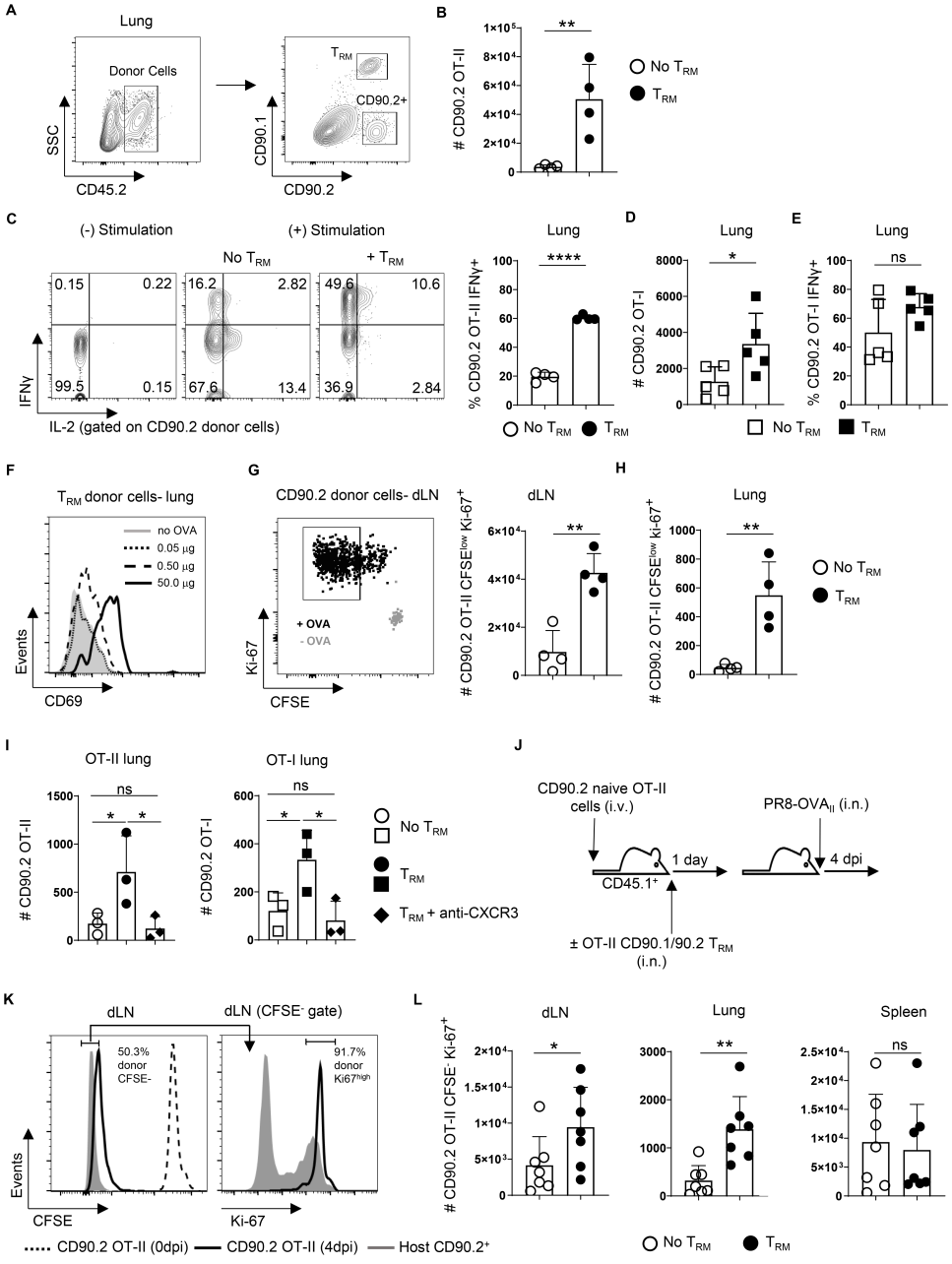

Figure 6: *Airway CD4 T_{RM} promote lung trafficking by newly activated T cells.* CD45.1^{+} B6 mice receiving naive CD45.2^{+} CD90.2^{+} OT-II cells i.v. with or without CD45.2^{+} CD90.1^{+}/CD90.2^{+} OT-II T_{RM} i.n. were then challenged i.n. with 50 µg of FITC-OVA. **(A)** Representative staining to identify donor OT-II subsets. **(B)** Number of naive OT-II responders in lungs after 4 days, **(C)**

representative IFNγ and IL-2 staining in mice without or without T_{RM}, and frequencies of $IFN\gamma^+$ cells derived from naive donors; n=4/group; 1 of 3 experiments. Separate mice received naive OT-I cells with or without OT-II T_{RM}. **(D)** Number of OT-I responders in lungs and **(E)** $IFN\gamma^+$ OT-I cells 4 days after FITC-OVA administration; n=5/group; 1 of 2 experiments. **(F)** Representative CD69 expression by T_{RM} 20 h after i.n. challenge with 50, 0.5., or 0.05 μg of FITC-OVA. **(G)** Representative Ki67 and CFSE expression by naive OT-II responders in dLNs of mice harboring OT-II T_{RM} given 0.5 μg FITC-OVA or PBS (left) and numbers of $CFSE^{low}Ki67^{high}$ cells in dLNs of mice harboring T_{RM} or not at day 3 (right), and **(H)** in lungs at day 4; n=4/group; 1 of 3 experiments for each timepoint. Mice receiving naive donor cells and T_{RM} were treated with CXCR3 blocking or control Ab prior to FITC-OVA administration. **(I)** Number of cells derived from naive OT-II (left) and OT-I (right) donors in lungs after 4 days; n=3/group; 1 of 2 experiments. **(J)** Unprimed mice receiving CFSE-labeled naive OT-II cells with or without T_{RM} were challenged with PR8-OVA_{II}. **(K)** Gating to identify effector cells derived from naive donors. **(L)** Number of $CFSE^-Ki67^{high}$ effectors at 4 dpi in stated organs; n=7/group; pooled from 2 experiments. Students t-test was used for pairwise comparison in all panels except (H) where one-way ANOVA with Tukey's multiple comparison was used.